

Constraint Propagation on GPU: A Case Study for the Bin Packing Constraint

Fabio Tardivo¹[0000-0003-3328-2174], Laurent Michel²[0000-0001-7230-7130], and
Enrico Pontelli¹[0000-0002-7753-1737]

¹ New Mexico State University {ftardivo,epontell}@nmsu.edu

² University of Connecticut laurent.michel@uconn.edu

Abstract. The Bin Packing Problem is one of the most important problems in discrete optimization, as it captures the requirements of many real-world problems. Because of its importance, it has been approached with the main theoretical and practical tools. Resolution approaches based on Linear Programming are the most effective, while Constraint Programming proves valuable when the Bin Packing Problem is a component of a larger problem.

This work focuses on the Bin Packing constraint and explores how GPUs can be used to enhance its propagation algorithm. Two approaches are motivated and discussed, one based on knapsack reasoning and one using alternative lower bounds. The implementations are evaluated in comparison with state-of-the-art approaches on different benchmarks from the literature. The results indicate that the GPU-accelerated lower bounds offers a desirable alternative to tackle large instances.

Keywords: Constraint Propagation · Bin Packing · Parallelism · GPU · Lower Bounds · Knapsack

1 Introduction

The *Bin Packing Problem (BPP)* consists of packing a set of items into the minimal number of bins, each with a fixed capacity. It has a fundamental role in logistics and resource management applications, making it one of the most important optimization problems.

The BPP is NP-Hard in the strong sense [16] and it is challenging to solve even for a fixed number of bins [19] or a constant number of different item sizes [17]. Over the last eighty years, numerous approaches to solve the BPP have been developed; we refer the interested reader to [9,31] for a comprehensive review. Techniques based on Integer Linear Programming (ILP) are highly effective and represent the state-of-the-art for solving the BPP. However, when the BPP is a component of a larger problem, applying such techniques becomes challenging, and *Constraint Programming (CP)* emerges as a valuable alternative. In these cases, the BPP appears in its decision version, where the items must be packed into a fixed number of bins.

The decision version of the BPP is modeled in CP using the `bin_packing` constraint [33]. Its filtering algorithm employs knapsack reasoning, to exclude or commit items to bins, and a feasibility check to prune the search if the remaining unpacked items cannot fit in the residual space of the bins. This check is performed using a lower bound on the number of bins necessary to pack the items. Typically, a combinatorial lower bound, named L_2 , is used, but [3] has shown that employing a tighter lower bound from the linear relaxation of a strong ILP formulation, known as Arc-Flow, greatly enhances the pruning.

This work explores the use of *Graphical Processing Units (GPUs)* for propagating the `bin_packing` constraint. The contributions of this paper include: 1) an enhanced feasibility check achieved by replacing L_2 with a collection of lower bounds; 2) the use of GPUs to parallelize the calculation of such lower bounds; 3) an empirical evaluation of sequential and GPU-accelerated lower bounds, compared to L_2 and to the lower bound from the Arc-Flow model.

The rest of the paper is organized as follows. Section 2 contains some general background about Constraint Satisfaction Problems and General-purpose computing on Graphics Processing Units (GPGPU). Section 3 summarizes related works on the `bin_packing` constraint. Section 4 details the design and implementation of the feasibility check enhanced with the GPU-accelerated lower bounds. Section 5 presents the results of our approach and the other techniques in the literature. Finally, Section 6 concludes the paper.

2 Background

2.1 Constraint Satisfaction/Optimization Problems

A Constraint Satisfaction Problem (CSP) is defined as $P = \langle V, D, C \rangle$, where $V = \{V_1, \dots, V_n\}$ is a set of *variables*, $D = \{D_1, \dots, D_n\}$ is a set of *domains*, and C is a set of *constraints*. A constraint $c \in C$, involves a set of m variables depending on its semantic. Such set is $vars(c) = \{V_{i_1}, \dots, V_{i_m}\} \subseteq V$, and defines a relation $c \subseteq D_{i_1} \times \dots \times D_{i_m}$. A *solution* is an assignment $\sigma : V \rightarrow \bigcup_{i=1}^n D_i$ such that $\sigma(V_i) \in D_i$ holds for every variable, and $\langle \sigma(V_{i_1}), \dots, \sigma(V_{i_m}) \rangle \in c$ holds for every constraint. A Constraint Optimization Problem (COP) is a quadruple $\langle V, D, C, f \rangle$ where $\langle V, D, C \rangle$ is a CSP and $f : D_1 \times \dots \times D_n \rightarrow \mathbb{R}$ is an *objective function* to be minimized. The goal is to find a solution σ that minimizes $f(\sigma(V_1), \dots, \sigma(V_n))$.

A *constraint solver* searches for solutions of a CSP/COP by alternating non-deterministic choices and constraints propagation. The first is employed to choose the next variable and which value, from its current domain, to assign to it. The second is a method to *filter* the domain of the variables, removing values that are not part of any solution. Non-deterministic choices are typically implemented through backtracking and heuristic decisions that follow an ordering among variables and values. Constraint propagation is commonly implemented through a queue that tracks constraints that need to be re-evaluated. When a value is removed from a variable's domain, the constraints involving such variable are enqueued. The re-evaluation consists of extracting the constraint from

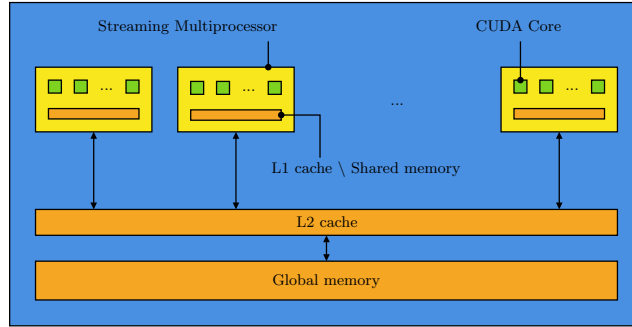


Fig. 1: High level architecture of a NVIDIA GPU.

the queue and applying the associated filtering algorithm or *propagator*. This iterative cycle continues until the queue is empty [21].

Different filtering algorithms offer different trade-offs between filtering power and computational complexity. Highly effective algorithms have been developed for *global constraints*. These constraints model a substantial portion of a CSP/-COP and naturally arise in various problems.

2.2 General-Purpose Computing on Graphics Processing Units

The computational power of modern GPUs facilitates the resolution of classes of problems that are too large to be effectively handled by CPUs. This advantage arises from GPUs massive parallelism, featuring thousands of computing units capable of efficiently processing vast amounts of data. However, to harness such computing power, it is crucial to employ approaches and algorithms that align with the underlying architecture of the GPU. Recent studies indicate that GPUs can be used for computational logic, including applications like SAT [8,7], ASP [11,12], and CP [34,35].

Most GPU-accelerated applications are developed using *CUDA*[24], a C/C++ API that exposes parallel computing primitives on NVIDIA GPUs. The part of an application executed by the CPU contains instructions for moving data to/from the GPU and offloading computation to the GPU.

The sample architecture of an NVIDIA GPU is illustrated in Figure 1. A modern high-end GPU is equipped with 128 *Streaming Multiprocessors (SM)*, each accommodating 128 computational units named *CUDA Cores*. In the lower and middle tiers of the memory hierarchy, there is the *global memory* with a capacity of 24 GB, and an *L2 cache* of 72 MB. At the top, there are 128 KB of fast memory serving as *L1 cache* and/or scratchpad memory (referred to as *shared memory*).

The CUDA execution model is *Single-Instruction Multiple-Thread (SIMT)*, where a C/C++ function known as *kernel* is executed by many threads. Each thread utilizes its own unique index to identify the data to use or to modify its control flow. When different threads follow distinct control flows, it leads to

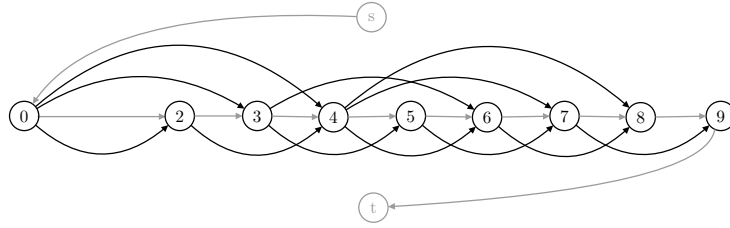


Fig. 2: Graph underlying the Arc-Flow model for an instance with $c = 9$ and $W = [4, 4, 3, 3, 2, 2]$.

thread divergence. In such scenarios, threads are serialized, potentially causing significant performance deterioration. Threads are organized into *blocks*, which are dispatched to the Streaming Multiprocessors. Each Streaming Multiprocessor executes the threads using its CUDA Cores, allowing efficient intra-block operations through shared memory. Communication between blocks is possible only through the use of global memory.

To successfully GPU accelerate an application, it is crucial to achieve good load balance, optimize memory access, and mitigate thread divergence [18]. This may require reformulating the problem to expose parallelism or exploiting shared memory to reduce the overhead of costly global memory accesses.

3 Bin Packing

Let $I = (c, W)$ be an instance of the Bin Packing Problem (BPP) with n items of weights $W = [w_1, \dots, w_n]$, and bins of capacity c . The *textbook* Integer Linear Programming (ILP) model is:

$$\begin{aligned}
 & \text{minimize} && \sum_{j=1}^n y_j \\
 & \text{subject to} && \sum_{i=1}^n w_i x_{ij} \leq cy_j && j = 1, \dots, n \\
 & && \sum_{j=1}^n x_{ij} = 1 && i = 1, \dots, n \\
 & && y_j \in \{0, 1\} && j = 1, \dots, n \\
 & && x_{ij} \in \{0, 1\} && i, j = 1, \dots, n
 \end{aligned}$$

where the Boolean variable y_j indicates whether the j^{th} bin is used and the variable x_{ij} indicates whether the i^{th} item is packed in the j^{th} bin.

A strong ILP formulation, known as *Arc-Flow* [4], is obtained by approaching the BPP from a graph-theoretical perspective. Given a BPP instance, a graph is built in such a way that arcs represent items, and a path from the source node s to the sink node t represents a set of items that can be packed into a bin (see fig. 2). A solution corresponds to a minimum flow that uses one arc

```

In:  $c, W = [w_1, \dots, w_n], k$ 
InOut:  $X = [x_1, \dots, x_n], L = [l_1, \dots, l_k]$ 
1 for  $j \leftarrow 1$  to  $k$  do // Basic filtering
2    $doLoadCoherence(j, X, W, L)$ 
3    $doBasicLoadTightening(j, X, W, L)$ 
4   for  $i \in \{i \mid j \in x_i \wedge |x_i| > 1\}$  do
5      $doBasicItemEliminationCommitment(i, j, X, W, L)$ 
6 for  $j \leftarrow 1$  to  $k$  do // Knapsack filtering
7   if  $\neg isBinPackable(j, X, W, L)$  then
8      $Fail$ 
9    $doKnapsackLoadTightening(j, X, W, L)$ 
10  for  $i \in \{i \mid j \in x_i \wedge |x_i| > 1\}$  do
11     $doKnapsackItemEliminationCommitment(i, j, X, W, L)$ 
12  $lb \leftarrow getLowerBound(c, W, k, X)$  // Feasibility check
13 if  $lb > k$  then
14    $Fail$ 
    
```

Algorithm 1: Simplified propagator for the `bin_packing` constraint.

for each $w \in W$. The ILP formulation of this flow problem has a strong linear relaxation, but it comes at the cost of a pseudo-polynomial number of variables and constraints.

In CP, the decision version of the BPP, where the items must be packed in at most k bins, is modeled as:

$$\begin{aligned}
 x_i &= \{1, \dots, k\} & i &= 1, \dots, n \\
 l_j &= \{0, \dots, c\} & j &= 1, \dots, k \\
 \text{bin_packing}([x_1, \dots, x_n], [w_1, \dots, w_n], [l_1, \dots, l_k])
 \end{aligned}$$

where the variable x_i represents the bins in which the i^{th} item can be packed, and the variable l_j represents the loads that the j^{th} bin can have.

The `bin_packing` constraint was introduced in [33] and a simplified version of its filtering algorithm is listed in algorithm 1. Following a brief description of each method:

Load coherence The minimum/maximum load of a bin is adjusted considering the total weight of the items and the load of the other bins.

Basic load tightening The minimum/maximum load of a bin is adjusted considering the sum of the items that are/can be packed in the bin.

Basic item elimination and commitment An item is committed to a bin if it is needed to reach a valid load. An item is excluded from a bin if packing it would lead to an excessive load.

Bin packability check A bin is considered packable if an approximated knapsack reasoning shows that it is possible to reach an admissible load.

Knapsack load tightening The minimum/maximum load of a bin is adjusted using an approximated knapsack reasoning.

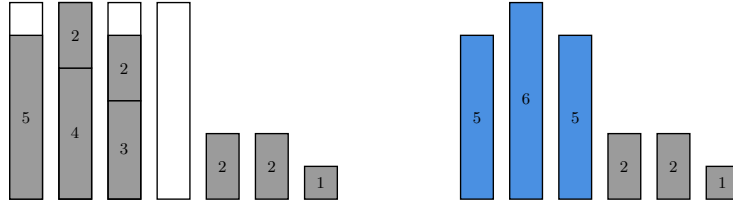


Fig. 3: Illustration of a partial packing (left) and its reduction (right). Virtual items are highlighted in blue.

Knapsack item elimination and commitment An item is committed or excluded from a bin using an approximated knapsack reasoning.

Feasibility check A partial packing is considered feasible if a lower bound on the number of bins does not exceed the available bins. The lower bound is calculated on a *reduced* instance derived from the current partial packing (see fig. 3). This instance is obtained by considering all the unpacked items and introducing one *virtual item* per bin to represent the items packed in that bin. Typically, the lower bound L_2 is used (see section 3.1).

The literature contains various extensions of the `bin_packing` constraint. The authors of [30,25,10] introduce and refine a *cardinality reasoning*, well suited when there are constraints on the number of items in each bin or when the items have similar weights. In [13], the lower bound is enhanced by considering *alternative reductions*. Finally, [3] achieves notable results using the lower bound derived from the linear relaxation of the *Arc-Flow* model.

3.1 Lower bounds

Given an instance $I = (c, W)$ of the BPP, a lower bound $L(I)$ estimates the minimum number of bins necessary to store the items. The simplest lower bound is referred to as L_1 , and is calculated as follows:

$$L_1(I) = \left\lceil \frac{1}{c} \sum_{w \in W} w \right\rceil$$

where the total weight of the items is divided by the bin capacity, and the ceiling function is applied. This approach is equivalent to naively packing the items, cutting those that do not entirely fit.

An improvement of L_1 , called L_2 , is introduced in [23] and addresses the cases where big items cannot be packed together. It is defined as:

$$L_2(I) = \max_{0 \leq \lambda \leq \frac{c}{2}} L_2(I, \lambda)$$

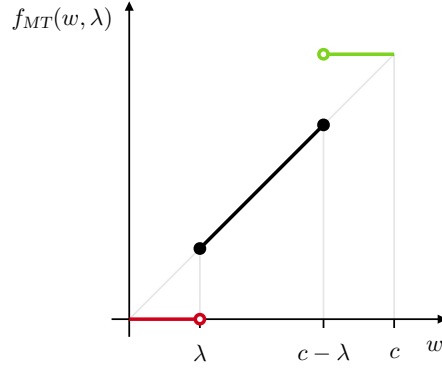


Fig. 4: Illustration of f_{MT} for $\lambda = c\frac{4}{15}$. Weights that have been increased/decreased are highlighted in green/red.

where

$$L_2(I, \lambda) = |W_1| + |W_2| + \max \left(0, \left\lceil \frac{1}{c} \left(\sum_{w \in W_3} w - \left(c|W_2| - \sum_{w \in W_2} w \right) \right) \right\rceil \right)$$

$$W_1 = \{w \mid w \in W \wedge c - \lambda < w\}$$

$$W_2 = \{w \mid w \in W \wedge \frac{c}{2} < w \leq c - \lambda\}$$

$$W_3 = \{w \mid w \in W \wedge \lambda \leq w \leq \frac{c}{2}\}$$

The lower bound $L_2(I, \lambda)$ is equivalent to first classifying the items as big (W_1), medium-big (W_2), and medium-small (W_3), while smaller items are ignored. Each of the big and medium-big items is packed in a different bin, since they are bigger than $\frac{c}{2}$. Finally, the medium-small items are packed as in L_1 , using the available space in the bins where there is a medium-big item before considering other bins. A direct implementation of L_2 is pseudo-polynomial, since $L_2(I, \lambda)$ has to be calculated $O(c)$ times. More efficient algorithms are described in [22,20], achieving linear complexity when the items are sorted in decreasing weight.

A general approach to enhance L_1 is based on *Dual Feasible Functions* (DFFs). These functions alter the weights of items. In the example below, $f_{MT}(w, \lambda)$ will either increase (when $w > c - \lambda$), decrease (when $w < \lambda$) or not change (when $\lambda \leq w \leq c - \lambda$) the original weight w . Note how increasing the weight to be c requires a dedicated bin for the item, while decreasing its weight to 0 says the item is ignored. The function is illustrated in fig. 4 and depends on an *integer* parameter λ :

$$f_{MT}(w, \lambda) = \begin{cases} c & \text{if } c - \lambda < w \\ w & \text{if } \lambda \leq w \leq c - \lambda \\ 0 & \text{if } w < \lambda \end{cases} \quad 0 \leq \lambda \leq \frac{c}{2}$$

The lower bound obtained by combining L_1 with f_{MT} is:

$$L_{MT}(I) = \max_{0 \leq \lambda \leq \frac{c}{2}} \left[\frac{1}{f_{MT}(c, \lambda)} \sum_{w \in W} f_{MT}(w, \lambda) \right]$$

and it is equivalent to L_2 [15]. Several other DFFs have been proposed, each with a different design. For brevity, we report only some of them and refer interested readers to [6,2] for a comprehensive review, and to [26,27] for further insights.

$$f_{RAD2}(w, \lambda) = \begin{cases} 0 & \text{if } w < \lambda \\ \lfloor \frac{c}{3} \rfloor & \text{if } \lambda \leq w \leq c - 2\lambda \\ \lfloor \frac{c}{2} \rfloor & \text{if } c - 2\lambda < w < 2\lambda \\ c - f_{RAD2}(c - w, \lambda) & \text{if } 2\lambda \leq w \end{cases}$$

$$f_{FS1}(w, \lambda) = \begin{cases} w\lambda & \text{if } \frac{w(\lambda+1)}{c} \in \mathbb{N} \\ \lfloor \frac{w(\lambda+1)}{c} \rfloor c & \text{otherwise} \end{cases}$$

$$f_{CCMI}(w, \lambda) = \begin{cases} 2 \lfloor \frac{c}{\lambda} \rfloor - 2 \lfloor \frac{c-w}{\lambda} \rfloor & \text{if } w > \frac{c}{2} \\ \lfloor \frac{c}{\lambda} \rfloor & \text{if } w = \frac{c}{2} \\ 2 \lfloor \frac{w}{\lambda} \rfloor & \text{if } w < \frac{c}{2} \end{cases}$$

$$f_{VB2}(w, \lambda) = \begin{cases} 2 \max(0, \lfloor \frac{c\lambda}{c} \rfloor - 1) - 2 \max(0, \lfloor \frac{c\lambda - w\lambda}{c} \rfloor - 1) & \text{if } w > \frac{c}{2} \\ \max(0, \lfloor \frac{c\lambda}{c} \rfloor - 1) & \text{if } w = \frac{c}{2} \\ 2 \max(0, \lfloor \frac{w\lambda}{c} \rfloor - 1) & \text{if } w < \frac{c}{2} \end{cases}$$

$$f_{BJ1}(w, \lambda) = \begin{cases} \lfloor \frac{w}{\lambda} \rfloor (\lambda - c \bmod \lambda) & \text{if } w \bmod \lambda \leq c \bmod \lambda \\ \lfloor \frac{w}{\lambda} \rfloor (\lambda - c \bmod \lambda) + w \bmod \lambda - c \bmod \lambda & \text{otherwise} \end{cases}$$

4 Design and Implementation

A strategy for leveraging the GPU in constraint propagation involves utilizing it for *strong filtering* at a reduced computational cost [35]. This approach can be extended to the **bin_packing** constraint by employing the GPU to perform a *complete knapsack reasoning* instead of an approximated one. With the exception of load coherence, all the basic and knapsack filterings in algorithm 1 can be performed using the Dynamic Programming (DP) approach presented in [36]. We have developed a GPU-accelerated implementation of this method, leveraging bitwise operations and processing each bin in parallel. Initial tests did not reveal significant differences in terms of explored nodes compared to the approximated reasoning. Scalability tests indicate that the GPU-accelerated implementation becomes faster than an optimized implementation of the approximated filtering when the number of bins is in the order of hundreds. Although the underlying DP tables are calculated very efficiently, this approach is hindered by the overhead


```

In:  $c, W = [w_1, \dots, w_n], k, X = [x_1, \dots, x_n]$ 
Out:  $lb$ 
1  $[w'_1, \dots, w'_r] \leftarrow getReduction(W, X)$ 
2  $W_R \leftarrow [w'_1, \dots, w'_r]$ 
3  $lb \leftarrow 0$ 
4 for  $f \in \{f_{MT}, f_{RAD2}, f_{FS1}, f_{CCMI}, f_{VB2}, f_{BJ1}\}$  do
5    $L_f \leftarrow 0$ 
6    $\underline{\lambda}, \bar{\lambda} \leftarrow getMinMaxParameter(f, c)$ 
7   for  $\lambda \leftarrow \underline{\lambda}$  to  $\bar{\lambda}$  do
8      $sum \leftarrow 0$  // Calculate  $L_1$ -like lower bound
9     for  $w \in W_R$  do
10       $sum \leftarrow sum + f(w, \lambda)$ 
11       $lb' \leftarrow \left\lceil \frac{sum}{f(c, \lambda)} \right\rceil$ 
12       $L_f \leftarrow max(L_f, lb')$ 
13    $lb \leftarrow max(lb, L_f)$ 
14   if  $lb > k$  then
15     return  $lb$ 
16 return  $lb$ 

```

Algorithm 2: Sequential DFFs-based *getLowerBound* function.

resulting from the transfer of the variables to/from the GPU, the identification of the items that can be packed in each bin, and the atomic commit/elimination of the items. These results lead us to discard this approach and stick with the standard approximated knapsack reasoning.

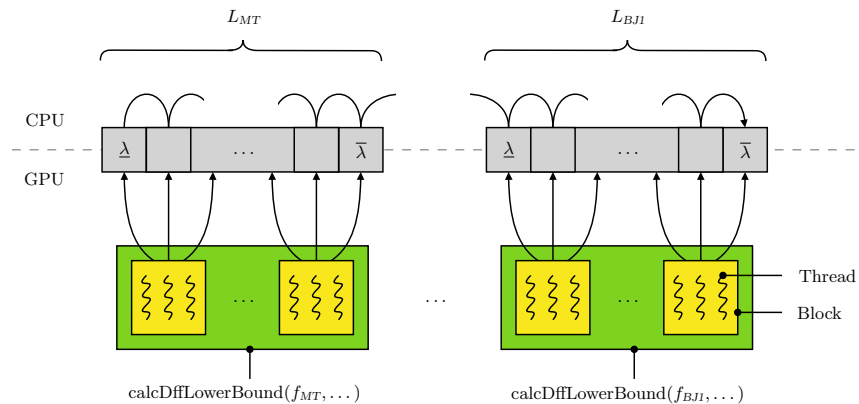
Another strategy to leverage the GPU in constraint propagation is to employ it to enhance the *pruning*. This translates into improving the feasibility check by utilizing the GPU to obtain the tightest lower bound at a reduced computational cost. Since the best lower bound is derived from a linear relaxation, it would reduce to solving a sparse linear system, a task notoriously hard to effectively accelerate by the GPU [18]. The next tightest lower bounds are obtained using Dual Feasible Functions (DFFs), and as demonstrated later in this section, these bounds are well-suited for GPU acceleration. The feasibility check can be easily adapted to make use of the DFFs-based lower bound listed in algorithm 2. The order in which the DFFs are considered impacts how quickly an infeasible partial packing is detected, and DFFs leading to a generally good lower bound should be prioritized. Table 1 presents a summary of the lower bounds derived from different DFFs on the Falkenauer and Scholl instances (see section 5). The column ‘Only Opt’/‘Only Best’ indicates the number of instances for which the DFF was the only one to lead to the optimal/best lower bound, while the ‘Sum’ column represents the sum of all the lower bounds calculated from the DFF. The optimal number of bins was found for 1305 out of 1370 total instances. The results confirm f_{CCMI} as the best overall function [6]. Interestingly, the generally weak f_{RAD2} proves effective when stronger functions are suboptimal [26].

DFF	Only Opt	Total Opt	Only Best	Total Best	Sum
f_{MT}	2	1151	0	55	120184
f_{RAD2}	10	189	0	36	105345
f_{FS1}	2	742	0	45	119504
f_{CCM1}	40	1219	1	60	120270
f_{VB2}	1	973	0	40	119786
f_{BJ1}	47	1101	0	50	120039

Table 1: Statistics of different DFF-based lower bounds.

Parallelization The GPU-accelerated feasibility check is outlined in algorithm 3. The core of the parallelization is a kernel named *calcDffLowerBound*, which is responsible for calculating the lower bounds derived from the different parameters of a DFF and keeping track of the tightest one (see algorithm 4). Concurrently running different copies of the kernel, each working with a different DFF, parallelizes the first outermost loop of algorithm 2. Using the threads to calculate the lower bounds parallelizes the second outermost loop (see fig. 5). Each thread is responsible for a distinct parameter value, requiring that $nThreads \geq \bar{\lambda} - \lambda + 1$. This condition is satisfied by launching each kernel with $\lceil \frac{\bar{\lambda} - \lambda + 1}{\#CS} \rceil$ blocks of size $\#CS$, where $\#CS$ is the number of CUDA Cores per Streaming Multiprocessors. With a bin capacity of 2000, a current high-end GPU achieves full parallelization of up to 8 DFFs, with a linear performance penalty for each additional DFF.

Implementation details The *calcDffLowerBound* kernel includes a couple of memory optimizations not represented in the pseudocode. First, each block initially copies $[w'_1, \dots, w'_r]$ into shared memory, ensuring fast accessibility for the subsequent lower bounds calculations. Second, the shared memory is also used to

**Fig. 5:** Sequential (top) and parallel (bottom) execution of the DFFs-based *getLowerBound* functions.

In: $c, W = [w_1, \dots, w_n], k, X = [x_1, \dots, x_n]$
Out: lb

```

1  $[w'_1, \dots, w'_r] \leftarrow getReduction(W, X)$ 
2  $W_R \leftarrow [w'_1, \dots, w'_r]$ 
3  $lb \leftarrow 0$ 
4  $cudaMemcpyCpuToGpu(c, W_R, lb)$  // Asynchronous APIs
5  $\underline{\lambda}, \bar{\lambda} \leftarrow getMinMaxParameter(f_{MT}, c)$ 
6  $cudaLaunchKernel(calcDffLowerBound, nThreads, [f_{MT}, \underline{\lambda}, \bar{\lambda}, c, W_R, k, lb])$ 
7 ...
8  $\underline{\lambda}, \bar{\lambda} \leftarrow getMinMaxParameter(f_{BJ1}, c)$ 
9  $cudaLaunchKernel(calcDffLowerBound, nThreads, [f_{BJ1}, \underline{\lambda}, \bar{\lambda}, c, W_R, k, lb])$ 
10  $cudaMemcpyGpuToCpu(lb)$ 
11  $waitGpu()$  // Synchronous API
12 return  $lb$ 

```

Algorithm 3: Parallel DFFs-based *getLowerBound* function.

In: $f, \underline{\lambda}, \bar{\lambda}, c, W_R = [w'_1, \dots, w'_r], k$
InOut: lb

```

1 if  $lb \leq k$  then
2    $L_f \leftarrow 0$  // Only one thread
3    $threadsBarrier()$ 
4    $tIdx \leftarrow getThreadIndex()$ 
5    $\lambda \leftarrow \underline{\lambda} + tIdx$ 
6   if  $\lambda \leq \bar{\lambda}$  then
7      $sum \leftarrow 0$  // Calculate  $L_1$ -like lower bound
8     for  $w \in W_R$  do
9        $sum \leftarrow sum + f(w, \lambda)$ 
10     $lb' \leftarrow \left\lceil \frac{sum}{f(c, \lambda)} \right\rceil$ 
11     $L_f \leftarrow max(L_f, lb')$  // Atomic operation
12     $threadsBarrier()$ 
13     $lb \leftarrow max(lb, L_f)$  // Only one thread, atomic operation

```

Algorithm 4: Pseudocode of the *calcDffLowerBound* kernel.

store L_f , allowing faster atomic operations that can run concurrently between blocks and reducing the number of atomic operations performed in the slower global memory.

Another optimization is employed at a higher level and consists of batching the memory operations and kernel launches to be called using a *single* API call. Depending on the instance, this technique provides a speedup up to 2x.

Finally, a note on numeric overflows. When the capacity is large, the intermediate values in the lower bound derived from f_{VB2} can exceed `UINT_MAX`. To address this problem, we limit the maximum parameter of f_{VB2} to $\left\lfloor \frac{\text{UINT_MAX}}{r \cdot \max(w'_1, \dots, w'_r)} \right\rfloor$.

5 Experiments

This section presents the results of a comparison between propagators that use different lower bounds for the feasibility check. We evaluate our implementation of L_2^3 , algorithm 2, algorithm 3, and the implementation from [3] which uses the Arc-Flow based lower bound. We refer to them as **L2**, **DFFs-CPU**, **DFFs-GPU**, **Arc-Flow**.

We select two classic BPP benchmarks from the literature [14,32], and generate new instances similar to the ones proposed in [5]. This results in a total of 1,922 instances organized as follows:

Falkenauer These instances are divided into two classes, each consisting of 80 instances. The ‘U’ instances contain items with weights uniformly distributed in the range $[20, 100]$, $n \in \{120, 250, 500, 1000\}$ and $c = 150$. The ‘T’ instances are more difficult, characterized by triplets of items that must be packed in the same bin in any optimal solution. For this class, $n \in \{60, 120, 249, 501\}$ and $c = 1000$.

Scholl These instances are divided into three sets of 720, 480, and 10 instances. Set 1 contains instances where the item weights are uniformly distributed to expect a number of items per bin not larger than three, $n \in \{50, 100, 200, 500\}$, $c \in \{100, 120, 150\}$. Set 2 contains more difficult instances where the item weights are uniformly distributed to expect between three and nine items per bin, $n \in \{50, 100, 200, 500\}$, $c = 1000$. Set 3 contains hard instances with weights uniformly distributed in the range $[20000, 35000]$, $n = 200$ and $c = 100000$.

Weibull These instances are based on the Weibull probability distribution. It can model various distributions found in different problem domains by adjusting the shape parameter $k > 0$ and the scale parameter $\lambda > 0$. We generated 92 sets of weights W with the parameters $n \in \{100, 200\}$, $k \in \{0.5, 0.6, \dots, 5.0\}$, and $\lambda = 1000$. For each set W , we generate 6 instances (c, W) with $c = \sigma \cdot \max(W)$ for $\sigma \in \{1.0, 1.2, \dots, 2.0\}$. The total number of instances is 552, with capacity ranging between 1300 and 92500.

The resolution procedure that we use is the same as in [33,3], where a minimum number of bins is established and an attempt to find a solution is made. If such a solution does not exist, the number of bins is increased, and a new attempt is made. All implementations use the *decreasing best fit* search heuristic. In this strategy, the items are considered in descending order of weight and assigned to the first bin within their domain that has the smallest residual capacity sufficient to accommodate the item. Additionally, two symmetry-breaking rules are applied on backtracking: first, the bin is removed from the domain of all items of the same size, and second, all the bins with the same load are removed from the domains of these items. Finally, a dominance rule is applied before a choice point: if an item completely fills the remaining capacity of a bin, it is assigned to that bin.

³ Algorithm with linear complexity time.

Benchmark	Lower Bound	Solved	Avg Time [s]	Tot Time [s]	Nodes
Falkenauer T	L2	38	11	408	1244813
	DFFs-CPU	58	64	3677	891909
	DFFs-GPU	58	21	1196	891909
	Arc-Flow	68	20	1327	5235
Falkenauer U	L2	31	20	628	8091399
	DFFs-CPU	59	60	3568	584459
	DFFs-GPU	60	59	3559	698451
	Arc-Flow	79	9	690	15990
Scholl 1	L2	640	7	4457	34421873
	DFFs-CPU	700	6	4374	3397547
	DFFs-GPU	703	6	3985	7901777
	Arc-Flow	717	3	2492	115520
Scholl 2	L2	336	5	1620	34401378
	DFFs-CPU	437	9	3950	596417
	DFFs-GPU	440	4	1951	2400806
	Arc-Flow	436	61	26800	278695
Scholl 3	L2	0	–	–	–
	DFFs-CPU	3	316	947	8221
	DFFs-GPU	3	1	3	8221
	Arc-Flow	0	–	–	–
Weibull	L2	375	70	26301	55122362
	DFFs-CPU	402	9	3432	722730
	DFFs-GPU	418	9	3652	35003432
	Arc-Flow	292	95	28022	11437

Table 2: Statistics for the solved instances of different lower bound methods.

The implementations L2, DFFs-CPU, and DFFs-GPU include additional techniques. First, another dominance rule is applied before a choice point: if at most one item fits in the residual capacity of a bin, the heaviest among such items is assigned to the bin [29]. Second, the feasibility check uses all three reductions described in [13]. Finally, the symmetry breaking described in [28] is enforced with an additional constraint. We discuss the impact of these techniques later in this section.

The experiments are performed with a time limit of 10 minutes to ensure a reasonable benchmark time. The system used for the tests is equipped with an Intel Core i7-10700K processor, 32 GB of RAM, and an NVIDIA GeForce RTX 3080. It runs Ubuntu 22.04, CUDA 11.8, Open JDK 11.0 and CPLEX 22.1.

5.1 Results and Analysis

The analysis focuses on instances solved within the time limit. Table 2 reports, for each approach and benchmark, the number of solved instances, the average time per solved instances, the total time to solve them, and the total number of visited nodes.

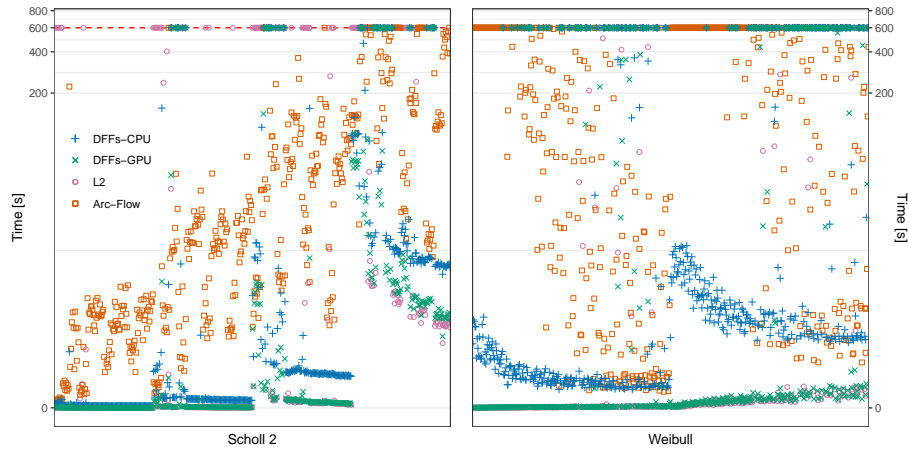


Fig. 6: Solve time for the Scholl 2 and Weibull instances. Note the logarithmic scale in the time axe. The DFFs-GPU points are colored in green.

The Falkenauer T instances highlight the contrast between fast but weak and slow but strong pruning. L_2 quickly solved almost half of the instances, while **Arc-Flow** solved 85% of them, taking on average twice the time per instance. The DFFs-based approaches fall in the middle, with the GPU-accelerated implementation being three times faster than the sequential version.

In the Falkenauer U and Scholl 1 instances, **Arc-Flow** demonstrated a good balance between speed and strength, solving almost all instances in a small amount of time. The DFFs-based approaches follow by number of solved instances, and L_2 comes last. Notice how the gap between **Arc-Flow** and the DFFs-based approaches shrinks from small (Falkenauer U) to larger (Scholl 1) bin capacities. The additional instances solved by **DFFs-GPU** compared to **DFFs-CPU** accounted for 15% (Falkenauer U) and 29% (Scholl 1) of the total solving time.

The results for the Scholl 2 instances (see fig. 6) show that **DFFs-GPU** is a competitive approach, solving a larger number of instances with the minimum average time. Closely following is **DFFs-CPU**, which is twice slower compared to the GPU version, and **Arc-Flow** that requires significantly more time. Finally, L_2 comes last, with a good average resolution time but fewer solved instances.

The Scholl 3 instances, characterized by their huge capacities, highlight the convenient trade-off between tight bounds and computational speed offered by DFFs. These approaches are the only ones able to solve some instances, with the GPU-accelerated implementation showing remarkable speedups.

The results obtained from the Weibull instances (see fig. 6) confirm the effectiveness of the DFFs-based approaches, especially for large bin capacity. **DFFs-GPU** solved more instances than its sequential counterpart, which accounts for 96% of the solving time. In third place is L_2 with a significantly larger average solving time, and last comes **Arc-Flow** with significantly fewer solved instances.

Version	Solved	Time [s]	Nodes
DFFs-GPU	1631	1847	4653344
DFFs-GPU-NoDom	1598	2515	16420684
DFFs-GPU-NoAltRed	1623	2597	12986578
DFFs-GPU-NoSymBrk	1591	5970	53424505

Table 3: Statistics for DFFs-GPU without optimizations.

In conclusion, the DFFs-based approaches offer an interesting tradeoff between pruning strength and computational speed that becomes more valuable as the bin capacity increases. The speedups provided by the GPU depend on both the capacity of the bins and the characteristics of the instance. As the calculation of the lower bound is the only GPU-accelerated operation, the benefits are proportional to the number of times the feasibility check is performed. This count can be significantly smaller than the number of propagator calls, since failures can occur earlier in the knapsack reasoning.

To assess the impact of the different optimizations we employed, an ablation study has been conducted on the instances solved by DFFs-GPU in less than 60 seconds. The results are presented in table 3, where each entry represents a version of DFFs-GPU with a disabled optimization. The most effective techniques are the dominance rule [33] and symmetry breaking [28]. In general, we strongly encourage the use of the latter since it is implementable as a standalone constraint and applicable to variations of the BPP with precedences or conflicts.

6 Conclusions and Future works

This paper discusses the Bin Packing Problem, presenting a feasibility check using different lower bounds derived from Dual Feasible Functions. While these lower bounds may not be the fastest or the tightest, the substantial parallelism offered by modern GPUs changes this position, making the approach effective, particularly for large problem instances.

This work raises several research questions that could be explored in future studies. From an analytical standpoint, it would be interesting to identify functions that lead to tight bounds in cases where the current ones fall short. On a practical note, a valuable extension would be to explore the effectiveness of multidimensional Dual Feasible Functions [1] on the Multidimensional/Vector Bin Packing Problem.

Acknowledgements

We would like to thank François Clautiaux and Maxence Delorme for their valuable feedbacks, Hadrien Cambazard for generously providing the original Arc-Flow implementation, and Jürgen Rietz for sharing insightful perspectives on Dual Feasible Functions.

References

1. Alves, C., de Carvalho, J.M.V., Clautiaux, F., Rietz, J.: Multidimensional dual-feasible functions and fast lower bounds for the vector packing problem. *Eur. J. Oper. Res.* **233**(1), 43–63 (2014). <https://doi.org/10.1016/J.EJOR.2013.08.011>
2. Alves, C., Clautiaux, F., de Carvalho, J.V., Rietz, J.: Dual-feasible functions for integer programming and combinatorial optimization. *EURO Advanced Tutorials on Operational Research*, Springer International Publishing, Basel, Switzerland (2016)
3. Cambazard, H., O’Sullivan, B.: Propagating the bin packing constraint using linear programming. In: Cohen, D. (ed.) *Principles and Practice of Constraint Programming - CP 2010 - 16th International Conference, CP 2010, St. Andrews, Scotland, UK, September 6-10, 2010. Proceedings. Lecture Notes in Computer Science*, vol. 6308, pp. 129–136. Springer (2010). https://doi.org/10.1007/978-3-642-15396-9_13
4. de Carvalho, J.M.V.: Exact solution of bin-packing problems using column generation and branch-and-bound. *Ann. Oper. Res.* **86**, 629–659 (1999). <https://doi.org/10.1023/A%3A1018952112615>
5. Castiñeiras, I., Cauwer, M.D., O’Sullivan, B.: Weibull-based benchmarks for bin packing. In: Milano, M. (ed.) *Principles and Practice of Constraint Programming - 18th International Conference, CP 2012, Québec City, QC, Canada, October 8-12, 2012. Proceedings. Lecture Notes in Computer Science*, vol. 7514, pp. 207–222. Springer (2012). https://doi.org/10.1007/978-3-642-33558-7_17
6. Clautiaux, F., Alves, C., de Carvalho, J.M.V.: A survey of dual-feasible and superadditive functions. *Ann. Oper. Res.* **179**(1), 317–342 (2010). <https://doi.org/10.1007/S10479-008-0453-8>
7. Collevati, M., Dovier, A., Formisano, A.: GPU parallelism for SAT solving heuristics. In: Calegari, R., Ciatto, G., Omicini, A. (eds.) *Proceedings of the CILC’22. CEUR Workshop Proceedings*, vol. 3204, pp. 17–31. CEUR-WS.org (2022)
8. Dal Palù, A., Dovier, A., Formisano, A., Pontelli, E.: CUD@SAT: SAT solving on GPUs. *J. Exp. Theor. Artif. Intell.* **27**(3), 293–316 (2015). <https://doi.org/10.1080/0952813X.2014.954274>
9. Delorme, M., Iori, M., Martello, S.: Bin packing and cutting stock problems: Mathematical models and exact algorithms. *European Journal of Operational Research* **255**(1), 1–20 (nov 2016). <https://doi.org/10.1016/j.ejor.2016.04.030>
10. Derval, G., Régim, J., Schaus, P.: Improved filtering for the bin-packing with cardinality constraint. *Constraints An Int. J.* **23**(3), 251–271 (2018). <https://doi.org/10.1007/S10601-017-9278-X>
11. Dovier, A., Formisano, A., Pontelli, E.: Parallel answer set programming. In: Hamadi, Y., Sais, L. (eds.) *Handbook of Parallel Constraint Reasoning*, pp. 237–282. Springer (2018). https://doi.org/10.1007/978-3-319-63516-3_7
12. Dovier, A., Formisano, A., Vella, F.: GPU-Based Parallelism for ASP-Solving. In: Hofstedt, P., Abreu, S., John, U., Kuchen, H., Seipel, D. (eds.) *Declarative Programming and Knowledge Management. Lecture Notes in Computer Science*, vol. 12057, pp. 3–23. Springer (2019). https://doi.org/10.1007/978-3-030-46714-2_1
13. Dupuis, J., Schaus, P., Deville, Y.: Consistency check for the bin packing constraint revisited. In: *Integration of AI and OR Techniques in Constraint Programming for Combinatorial Optimization Problems*, pp. 117–122. Springer Berlin Heidelberg (2010). https://doi.org/10.1007/978-3-642-13520-0_15

14. Falkenauer, E.: A hybrid grouping genetic algorithm for bin packing. *J. Heuristics* **2**(1), 5–30 (1996). <https://doi.org/10.1007/BF00226291>
15. Fekete, S.P., Schepers, J.: New classes of fast lower bounds for bin packing problems. *Math. Program.* **91**(1), 11–31 (2001). <https://doi.org/10.1007/S101070100243>
16. Garey, M.R., Johnson, D.S.: *Computers and Intractability: A Guide to the Theory of NP-Completeness*. W. H. Freeman (1979)
17. Goemans, M.X., Rothvoss, T.: Polynomiality for bin packing with a constant number of item types. *J. ACM* **67**(6), 38:1–38:21 (2020). <https://doi.org/10.1145/3421750>
18. Hwu, W.M.W., Kirk, D.B., El Hajj, I.: *Programming Massively Parallel Processors: A Hands-on Approach*. Morgan Kaufmann (2022), <https://shop.elsevier.com/books/programming-massively-parallel-processors/hwu/978-0-323-91231-0>
19. Jansen, K., Kratsch, S., Marx, D., Schlotter, I.: Bin packing with fixed number of bins revisited. *J. Comput. Syst. Sci.* **79**(1), 39–49 (2013). <https://doi.org/10.1016/j.jcss.2012.04.004>
20. Korf, R.E.: A new algorithm for optimal bin packing. In: Dechter, R., and Richard S. Sutton, M.J.K. (eds.) *Proceedings of the Eighteenth National Conference on Artificial Intelligence and Fourteenth Conference on Innovative Applications of Artificial Intelligence, July 28 - August 1, 2002, Edmonton, Alberta, Canada*. pp. 731–736. AAAI Press / The MIT Press (2002), <http://www.aaai.org/Library/AAI/2002/aaai02-110.php>
21. Mackworth, A.K.: Consistency in networks of relations. *Artif. Intell.* **8**(1), 99–118 (1977). [https://doi.org/10.1016/0004-3702\(77\)90007-8](https://doi.org/10.1016/0004-3702(77)90007-8)
22. Martello, S., Toth, P.: *Knapsack Problems: Algorithms and Computer Implementations*. John Wiley & Sons, Inc. (1990)
23. Martello, S., Toth, P.: Lower bounds and reduction procedures for the bin packing problem. *Discret. Appl. Math.* **28**, 59–70 (1990). [https://doi.org/10.1016/0166-218X\(90\)90094-S](https://doi.org/10.1016/0166-218X(90)90094-S)
24. Nvidia Team: CUDA, <https://developer.nvidia.com/cuda-toolkit>
25. Pelsser, F., Schaus, P., Régim, J.: Revisiting the cardinality reasoning for binpacking constraint. In: Schulte, C. (ed.) *Principles and Practice of Constraint Programming - 19th International Conference, CP 2013, Uppsala, Sweden, September 16-20, 2013. Proceedings. Lecture Notes in Computer Science*, vol. 8124, pp. 578–586. Springer (2013). https://doi.org/10.1007/978-3-642-40627-0_43
26. Rietz, J., Alves, C., de Carvalho, J.M.V.: Theoretical investigations on maximal dual feasible functions. *Oper. Res. Lett.* **38**(3), 174–178 (2010). <https://doi.org/10.1016/J.ORL.2010.01.002>
27. Rietz, J., Alves, C., de Carvalho, J.M.V.: Worst-case analysis of maximal dual feasible functions. *Optim. Lett.* **6**(8), 1687–1705 (2012). <https://doi.org/10.1007/S11590-011-0359-2>
28. Salem, K.H., Kieffer, Y.: An experimental study on symmetry breaking constraints impact for the one dimensional bin-packing problem. In: Ganzha, M., Maciaszek, L.A., Paprzycki, M. (eds.) *Proceedings of the 2020 Federated Conference on Computer Science and Information Systems, FedCSIS 2020, Sofia, Bulgaria, September 6-9, 2020. Annals of Computer Science and Information Systems*, vol. 21, pp. 317–326 (2020). <https://doi.org/10.15439/2020F19>
29. Schaus, P.: *Solving Balancing and Bin-Packing problems with Constraint Programming*. Ph.D. thesis, University of Louvain (2009), http://cp2013.a4cp.org/sites/default/files/pierre_schaus_-_mr.pdf

30. Schaus, P., Régim, J., Schaeren, R.V., Dullaert, W., Raa, B.: Cardinality reasoning for bin-packing constraint: Application to a tank allocation problem. In: Milano, M. (ed.) Principles and Practice of Constraint Programming - 18th International Conference, CP 2012, Québec City, QC, Canada, October 8-12, 2012. Proceedings. Lecture Notes in Computer Science, vol. 7514, pp. 815–822. Springer (2012). https://doi.org/10.1007/978-3-642-33558-7_58
31. Scheithauer, G.: Introduction to Cutting and Packing Optimization. Springer International Publishing (2018). <https://doi.org/10.1007/978-3-319-64403-5>
32. Scholl, A., Klein, R., Jürgens, C.: Bison: A fast hybrid procedure for exactly solving the one-dimensional bin packing problem. *Comput. Oper. Res.* **24**(7), 627–645 (1997). [https://doi.org/10.1016/S0305-0548\(96\)00082-2](https://doi.org/10.1016/S0305-0548(96)00082-2)
33. Shaw, P.: A constraint for bin packing. In: Principles and Practice of Constraint Programming – CP 2004, pp. 648–662. Springer Berlin Heidelberg (2004). https://doi.org/10.1007/978-3-540-30201-8_47
34. Tardivo, F., Dovier, A., Formisano, A., Michel, L., Pontelli, E.: Constraint propagation on GPU: A case study for the AllDifferent constraint. *Journal of Logic and Computation* p. exad033 (06 2023). <https://doi.org/10.1093/logcom/exad033>
35. Tardivo, F., Dovier, A., Formisano, A., Michel, L., Pontelli, E.: Constraint propagation on GPU: A case study for the cumulative constraint. In: Ciré, A.A. (ed.) Integration of Constraint Programming, Artificial Intelligence, and Operations Research - 20th International Conference, CPAIOR 2023, Nice, France, May 29 - June 1, 2023, Proceedings. Lecture Notes in Computer Science, vol. 13884, pp. 336–353. Springer (2023). https://doi.org/10.1007/978-3-031-33271-5_22
36. Trick, M.A.: A dynamic programming approach for consistency and propagation for knapsack constraints. *Ann. Oper. Res.* **118**(1-4), 73–84 (2003). <https://doi.org/10.1023/A:1021801522545>